DOI:
10.1016/j.molliq.2022.119963

Document Version
Publisher's PDF, also known as Version of record

Journal of Molecular Liquids 364 (2022) 119963

Contents lists available at ScienceDirect

Journal of Molecular Liquids

journal homepage: www.elsevier.com/locate/molliq

On the interactions of diols and DMPC monolayers

Natasha H. Rhys [a], David J. Barlow [b], M. Jayne Lawrence [b,*], Christian D. Lorenz [a,*]

[a] Biological Physics & Soft Matter Group, Department of Physics, Strand, London WC2R 2LS, United Kingdom
[b] Division of Pharmacy and Optometry, School of Health Sciences, Faculty of Biology, Medicine and Health, University of Manchester, Stopford Building, Oxford Road, Manchester M13 9PL, United Kingdom

ARTICLE INFO

Article history:
Received 28 March 2022
Revised 23 July 2022
Accepted 26 July 2022
Available online 29 July 2022

Keywords:
DMPC
Diols
Molecular dynamics simulations
Solvent-mediated interactions

ABSTRACT

The interactions of lipid molecules with various solvent molecules is of utmost importance in the formulation of various drug delivery and personal care formulations. In this manuscript, a series of all-atom molecular dynamics simulations were used to investigate how the structural and interfacial properties of a DMPC (1,2-dimyristoyl-sn-glycero-3-phosphocholine) monolayer change when interacting with a range of diols that have varying carbon chain lengths and patterns of hydroxylation. In comparison to water, we find that all of the diols studied result in a more disordered and thinner monolayer. Additionally, we find that the shorter diols with the hydroxyl groups on neighbouring carbons (1,2-ethanediol and 1,2-propanediol) are able to penetrate deeper into the head group region of the lipid monolayers and as a result significantly disorder and thin the monolayers. Like water, we find that the diols also form hydrogen-bonded networks that connect the DMPC head groups in neighbouring molecules. Interestingly, we find that the number of butanediol molecules that form these solvent-mediated interactions between the DMPC head groups is directly affected by the distribution of the hydroxyl groups within the diol molecules. The results presented here provide a mechanistic description of how the chemistry of diol solvent molecules will affect the structural and interfacial properties of lipid structures in solution.

1. Introduction

The effect that solvents and co-solvents have on the structural and dynamic properties of lipid molecules in self-assembled structures is of significant interest for a variety of applications ranging from drug delivery and personal care formulations to cryopreservation. As water is the most biologically and industrially relevant solvent, there have been a large number of investigations of the interactions between water and lipid head groups [1–9]. There also have been numerous studies of the effects of a range of co-solvents on the interfacial behaviour and structural properties of lipid monolayers and bilayers [10–26].

Polyhydroxylated co-solvents such as 1,2-propanediol, 1,2-ethanediol and glycerol have all been used as cryoprotectants with less toxicity than dimethyl sulfoxide [27]. Likewise, polyols, also known as sugar alcohols or hydrogenated carbohydrates, are widely used in formulations in the food, pharmaceutical and cosmetic industries in order to impart a variety of functionalities [28–34,22,35,36]. While a large number of studies investigating the interactions between lipids and amphiphilic compounds can be found in the scientific literature, there has been a relatively limited number of studies of the effects of polyhydroxylated compounds with lipids. The majority of the studies that have been published exploring the interactions of polyhydroxylated compounds and lipids have consisted of aqueous solutions of polyhydroxylated compounds. Budziak et al. studied the effect of varying the chain length of the polyols (e.g. erythritol, xylitol and mannitol) in aqueous solution on their interactions with 1,2-dimyristoyl-*sn*-glycero-3-phosphocholine (DMPC) monolayers [25]. They found that these polyols do not incorporate into the hydrophobic part of the lipid monolayer and they thus have little effect on the molecular organisation within DMPC lipid monolayers, and minimal effect on the main phase transition temperature of the DMPC monolayer.

Dickey and Faller investigated how alcohols (e.g. ethanol, 1-propanol and 1-butanol) at various concentrations in water affect the properties of DPPC lipid bilayers [37]. They showed that the length of the alkyl chains of the alcohol molecules has a greater

* Corresponding authors.
E-mail addresses: natasha.rhys@kcl.ac.uk (N.H. Rhys), david.barlow@manchester.ac.uk (D.J. Barlow), jayne.lawrence@manchester.ac.uk (M.J. Lawrence), chris.lorenz@kcl.ac.uk (C.D. Lorenz).
URLs: https://www.kcl.ac.uk/people/natasha-rhys (N.H. Rhys), https://www.research.manchester.ac.uk/portal/jayne.lawrence.html (M.J. Lawrence), https://www.kcl.ac.uk/people/chris-lorenz (C.D. Lorenz).

https://doi.org/10.1016/j.molliq.2022.119963
0167-7322/

impact than the concentration of the alcohols on the nature of the hydrogen bonding between the lipid molecules and the alcohol molecules, which is consistent with the small-angle neutron study conducted by Kondela et al. [38]. In these studies, they showed that the alcohol molecules inserted their tails into the hydrophobic core of the lipid bilayers which suggests that the amphiphilic alcohols preferentially orient themselves such that their tails are parallel to the lipid acyl chains. As a result, they found that the insertion depth of the alcohol molecules is more dependent on the alkyl tail length of the alcohol than its concentration.

While there have been systematic investigations of the chain length dependence on the interaction between aqueous mixtures of monoalcohols and polyols with PC lipid membranes, there has been no such investigation for diols. In this manuscript, we use all-atom molecular dynamics (MD) simulations to elucidate the interactions between pure diol solutions ranging from 1,2-ethanediol to butanediol with DMPC monolayers. Through this, we investigate how the distribution of hydroxyl groups within propanediol and butanediol affects these interactions. In doing so, we explore the effect of these solvents on the structural and interfacial properties of the lipid monolayers. Finally, we investigate the hydrogen bonding between the diols and the lipids as well as the solvent mediated hydrogen bonded structures that form at the lipid interface, which have a direct impact on the structural properties of the membranes.

2. Methods

A series of all-atom MD simulations have been used to study the effects of various diols on the structural and interfacial properties of a DMPC lipid monolayer. For each solvent, we have created two monolayers containing 100 lipid molecules which are separated by a layer of the solvent. In doing so, we have studied seven different solvents: (i) water (12030 molecules), (ii) 1,2-ethanediol (4142 molecules), (iii) 1,2-propanediol (3165 molecules), (iv) 1,3-propanediol (3226 molecules), (v) 1,2-butaneldiol (2570 molecules), (vi) 1,3-butanediol (2596 molecules) and (vii) 1,4-butanediol (2621 molecules). In order to create these monolayer systems we first equilibrated a DMPC bilayer solvated by each solvent, and then separated the two leaflets such that they created two isolated monolayers (as shown in Fig. 1).

2.1. Simulation Protocol

The CHARMM-GUI Bilayer Builder was used to generate an initial DMPC bilayer with 100 lipids per leaflet.[39–42]. Then Packmol [43] was used to generate a slab of each solvent such that the interfaces of the two leaflets were separated by $\sim$ 60 Å. Each bilayer was then equilibrated as prescribed by the input files produced by the CHARMM-GUI Membrane Builder [44]. After the various stages of equilibration, the production simulation prescribed by CHARMM-GUI was performed for 500 ns in order to equilibrate the area per lipid of each membrane/solvent system.

The bilayers were divided into two monolayers separated by each of the respective solvents (Fig. 1B). The potential energy was again minimised using the steepest descent algorithm, then the systems were run under NVT for 100 ns using a 2.0 fs timestep with a Nosé-Hoover thermostat with a target temperature of 300 K and a time constant of 1.0 ps. All simulations used a cutoff of 1.2 nm for Lennard-Jones forces and a switching function with an inner cutoff of 1.0 nm to ensure the interactions go to zero continuously. The particle–particle-particle mesh algorithm was used to calculate the electrostatic interactions with a real-space cutoff of 1.2 nm.

For the monolayer simulations, the unit cell was periodic only in the x and y dimensions. As such, to produce a pseudo-2d Ewald summation, force and potential corrections were applied in the z dimension. All simulations were run using the CHARMM36 force field as it is implemented within the LAMMPS molecular dynamics package. [45] The production simulation of the monolayers was used for the analysis reported in this manuscript.

2.2. Simulation Analysis

All analyses were performed with in-house Python scripts using MDAnalysis[46,47], Lipyphilic[48] and Freud.[49]. The hydrogen bond analysis tool of MDAnalysis was used for finding hydrogen bonds, such that a hydrogen bond is defined by the distance between donor and acceptor atoms being less than 3.0 Å and the angle formed by the donor atom, the hydrogen atom and the acceptor atom is greater than 150°.[50].

In order to investigate if the different solvents encourage the PC headgroups of the lipid molecules to take a unique conformation, we have measured the angle (θ) that is formed by the vector con-

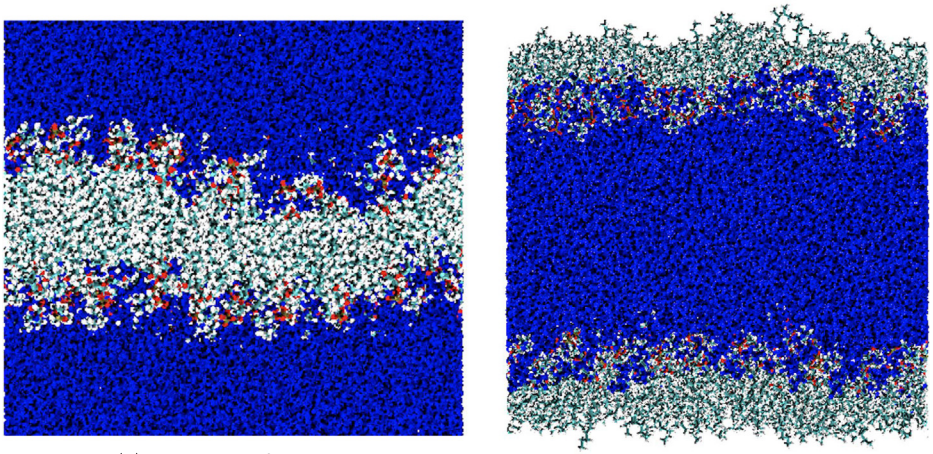

(a) Bilayer configuration

(b) Monolayer configuration

Fig. 1. Representative snapshots of (a) DMPC bilayer in contact with 1,2-ethanediol and (b) DMPC monolayers in contact with 1,2-ethanediol. The lipids are shown such that the carbon (cyan), oxygen (red), hydrogen (white), nitrogen (blue), and phosphorus (brown) atoms are all coloured differently. The 1,2-ethanediol molecules are then represented as a blue molecule.

necting the phosphorus and nitrogen atoms within the PC head group and the vector normal to the monolayer/solvent interface ($(0,0,-1)$ for the top monolayer, $(0,0,1)$ for the bottom monolayer).

The MD trajectories for all monolayer systems were further analyzed using the software ANGULA.[51,52] Here, a set of orthonormal coordinates was assigned to the solvent molecule hydroxyl atoms (see Figure S2) to assess the 3-dimensional arrangement of solvent molecules through the production of Spatial Density Maps (SDMs). The results were obtained through analyzing frames of number comparable to those used in ANGULA analyses on previous studies of 1,2-propanediol[53] and other lipid molecules[6,23,7], with the orthonormal axes used the same as those incorporated in the study of the solvation of the C_3-PC lipid head group.[23] The number of frames used were: water - 5000, 1,2-ethanediol - 5810, 1,2-propanediol - 5032, 1,3-propanediol - 5335, 1,2-butanediol - 3388, 1,3-butanediol - 5541 and 1,4-butanediol - 5507. The maps show the location of molecule hydroxyls around a central group, with the scale bar representing the density of atoms per Å^3 found within the distance covered by the first coordination shell and at a specified percentage.

3. Results

3.1. Area per lipid

We have used a Voronoi tessellation of each monolayer to calculate the interfacial area occupied by each DMPC molecule when interacting with the various solvents. The probability distribution of the area per DMPC molecules is shown in Fig. 2, and the average and standard deviation of the area per DMPC in each system are shown in Table 1. The DMPC monolayers interacting with 1,2-butanediol, 1,3-butanediol and 1,4-butanediol all have quite similar areas per lipid, averaging ca. 58 Å^2. The distribution of the area per lipid values has larger tails for the 1,2-butanediol than for 1,3-butanediol and 1,4-butanediol, while the monolayers interacting with 1,3-butanediol and 1,4-butanediol have nearly identical distributions of area per DMPC. The average area per DMPC in the 1,3-propanediol system is slightly larger ($\sim$ 60 Å^2) than that found for the butanediol systems, and the peak of the distribution is shifted slightly to larger values but the width of the distribution is the same as in 1,3-butanediol and 1,4-butanediol. The largest average areas per DMPC we observe are in the 1,2-ethanediol and 1,2-propanediol systems ($\sim$ 80 Å^2). In the distributions of the area per lipid values, we observe that while 1,2-propanediol shares the same location for the peak in its distribution as 1,2-ethanediol, the distribution for 1,2-propanediol is significantly more broader than for 1,2-ethanediol.

3.2. Monolayer thickness

In order to describe the thickness of the monolayers, we determined the minimum and maximum z-coordinates of the atoms in each DMPC molecule, and then took the difference of these two values. Then we averaged this thickness of the DMPC molecules over all molecules in the monolayers and over all configurations in the trajectory. Similarly we calculated the thickness of the sub-layers within the monolayers that are occupied by the lipid head groups and the hydrocarbon chains. The probability distributions of the DMPC monolayer thicknesses are shown in Fig. 3. We see that there is an inverse relationship between the area per lipid molecule and the thickness of the lipid monolayers on the various solvents (see Table 1). The difference in the thickness of the monolayers in the different diols is due to differences in thickness of the hydrocarbon tails sub-layer. This is due to the fact that when the lipid molecules are close packed, the tails are relatively vertical in relation to the z-axis. Meanwhile, those solvents (1,2-ethanediol & 1,2-propanediol) that result in the lipid molecules exhibiting larger areas per lipid also result in the thinner monolayers ($\sim$ 19 Å, see Table 1) as there is more free volume within the monolayers to allow the lipid tails to tilt. Therefore the hydrocarbon tails of the lipid molecules with these solvents are less extended in the direction normal to the monolayer's interface.

3.3. Lipid order

In order to measure the internal structure of the monolayers, we have calculated the average lipid order parameter, S_{cd}, for the DMPC molecules comprising the monolayers interacting with the various solvents. The average lipid order parameter $\langle S_{cd}\rangle$ for the DMPC molecules is calculated as

$$\langle S_{cd}\rangle = \frac{1}{2}\langle 3\cos^2\theta_{CD} - 1\rangle \quad (1)$$

where θ_{CD} is the angle formed between the vector consisting of a carbon and its bonded hydrogen in the lipid tail and the vector normal to the water/monolayer interface. Fig. 4 shows the average values for each carbon in the sn1 and sn2 tails of the DMPC lipids in each system. From these plots we see that the lipid monolayers which were found to have the smallest area per lipid and largest lipid monolayer thickness (1,2-butanediol, 1,3-butanediol, 1,4-butanediol, 1,3-propanediol & water), also are found to be the most ordered. In the thinner monolayers that are formed in contact with 1,2-ethanediol and 1,2-propanediol, however, where the DMPC area per molecule is larger, the lipid acyl chains are less ordered.

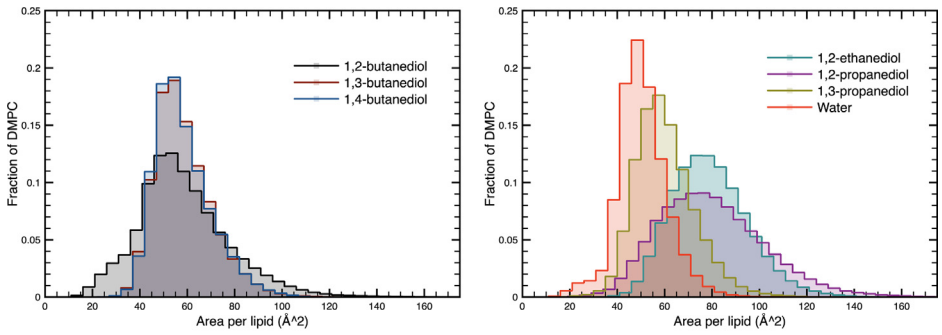

Fig. 2. Probability distribution of the area per DMPC molecule in the monolayers in contact with (a) 1,2-butanediol, 1,3-butanediol and 1,4-butanediol and (b) 1,2-ethanediol, 1,2-propanediol, 1,3-propanediol and water.

Table 1
Physical properties of the DMPC monolayers interacting with the various solvents. Average and standard deviation of the area per DMPC (Å^2) & the thickness (Å) of the DMPC monolayer, head group and tail.

Solvent	Area (Å^2)	Thickness (Å) Monolayer	Head group	Tail	θ_{PN} (°)
Water	51 ± 12	23.4 ± 2.7	7.6 ± 1.8	15.8 ± 1.9	90.2 ± 34.7
1,2-ethanediol	79 ± 16	19.3 ± 2.8	6.5 ± 1.6	12.8 ± 2.3	90.0 ± 26.3
1,2-propanediol	80 ± 22	19.4 ± 3.1	6.1 ± 1.7	13.3 ± 2.5	90.7 ± 28.5
1,3-propanediol	60 ± 13	21.2 ± 2.4	6.7 ± 1.7	14.5 ± 1.9	89.7 ± 26.5
1,2-butanediol	59 ± 20	21.1 ± 2.7	6.5 ± 1.6	14.6 ± 2.1	90.0 ± 26.5
1,3-butanediol	58 ± 12	21.5 ± 2.2	6.6 ± 1.5	14.9 ± 1.8	90.0 ± 24.5
1,4-butanediol	58 ± 12	21.5 ± 2.3	6.7 ± 1.6	14.8 ± 1.8	90.0 ± 26.7

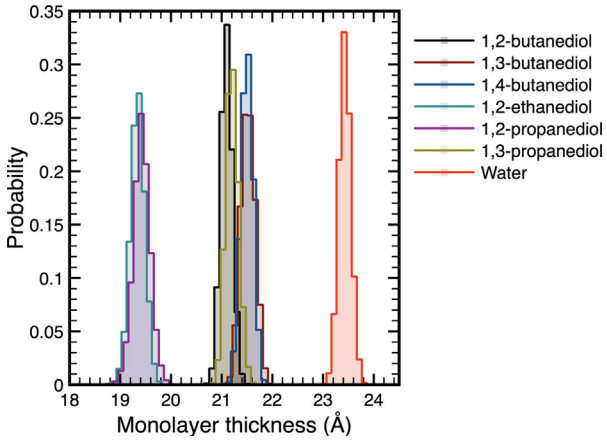

Fig. 3. Probability distribution of the thickness of the DMPC monolayers in each solvent system.

3.4. Diffusion of DMPC lipid molecules

Figure S4 shows the mean-square displacement in the $x-y$ plane for the DMPC lipids in each of the solvent systems. Table 2 shows the diffusion coefficients that have been measured from each of those plots. The value of the diffusion coefficient that has been calculated for the lipids in the DMPC monolayer in water is consistent with that found experimentally for pure DLPC monolayers [54].

The DMPC lipid molecules move significantly slower in the various diols than in water. Generally, the diffusion coefficient of the lipids within the various diols increases as the area per lipid of the DMPC in the solvents increases.

3.5. Orientation of the DMPC head groups

The distribtuion of the orientation of the P-N vector within the DMPC head group for each system is shown in Figure S3, and the

Table 2
Diffusion coefficients (in $x-y$ plane) of the DMPC molecules interacting with the various solvents. Average and standard error of the diffusion coefficients are reported.

Solvent	Diffusion coefficients (10^{-7} cm^2 s^{-1})
Water	37.0 ± 0.1
1,2-ethanediol	8.6 ± 1.1
1,2-propanediol	5.6 ± 0.9
1,3-propanediol	2.4 ± 0.4
1,2-butanediol	5.4 ± 0.6
1,3-butanediol	8.2 ± 0.9
1,4-butanediol	2.2 ± 0.4

average tilt angles are displayed in Table 1. The average orientation of the P-N vector in each solvent is approximately 90°. Similar headgroup tilt angle distributions have been reported in previous simulation studies of DMPC bilayers at 25°C [55,56] and for previous simulation [57] and experimental [58–61] studies of DPPC monolayers.

The distribution of angles is significantly broader for the DMPC lipids interacting with water than with any of the diols. The distribution of θ_{PN} for the diols are such that they have heavier tails for the angles representing the head groups being more extended into the solvent phase ($\theta_{PN} < 90°$).

3.6. Solvation of the DMPC head groups

In order to quantify the solvation of the DMPC head groups in each system, we have calculated radial distribution functions (rdfs, $g(r)$) of the nitrogen (NTL, Fig. S1) within the choline group, the phosphorus atom in the phosphate group (PTL, Fig. S1) and the double bonded oxygen (OE2, Fig. S1) in the ester groups of the DMPC lipids with the various oxygens and hydrogens of the various solvent molecules. These rdfs are shown in the SI (Figs. S5 - S35) and the nearest and second neighbour distances and coordination numbers are summarised in tables in the SI (Tables S1 - S9). Additionally, we have calculated the spatial density maps for the interactions of the various solvents around the same three

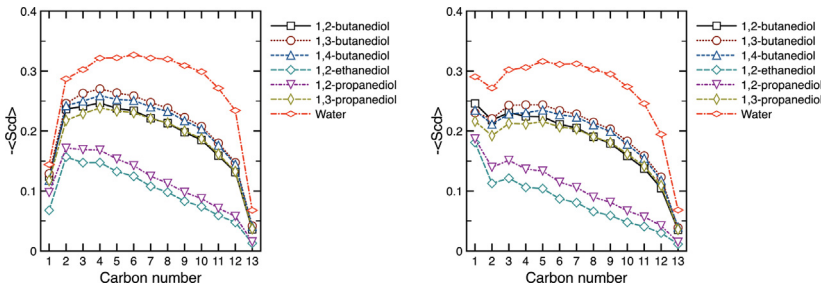

(a) sn1 tail (b) sn2 tail

Fig. 4. Lipid order parameters for the (a) sn1 and (b) sn2 tails of the DMPC lipid molecules in the monolayers for the various diol systems.

parts of the DMPC head groups, and those are also presented in the SI (Figs. S36 - S49). In Fig. 5, we summarise these interactions with the rdfs for the oxygen atoms in the hydroxyl groups of the different solvent molecules around the three reference atoms in the DMPC head group. In general, one can gain information about the structure of the solvation shells around a reference atom from the co-ordinates of the maxima and minima in the $g(r)$ distributions. Additionally the amount of solvent present within a given shell can be determined by integrating the rdfs between a pair of distances representing the extent of that solvation shell.

In Fig. 5a, the magnitudes of the first peaks of the various solvents vary, however the most notable difference in the various solvents is the location of the first minimum, which is the definition commonly used to define the maximum distance from the reference atom that is still considered part of the first solvation shell. As can be seen in Tables S1, S2 & S9, the distance to the first minimum, $r_{c,1}$, ranges from 5.25 Å for 1,2-ethanediol to 5.85 Å for 1,4-butanediol and 5.95 Å for water. As can be seen by looking at the rdfs for the individual oxygen atoms in the two hydroxyl groups in each of the diols that we have investigated (Figs. S5a, S10a, S15a, S20a, S25a & S30a), the spacing between the two hydroxyl groups within the molecule has a direct effect on the first minimum of each oxygen. Therefore when averaged together in Fig. 5a, these differences manifest in the differing values for the first minima observed. The electrostatic interaction between the negatively charged oxygen of the water molecule and the postively charged choline group results in a larger first solvation shell and therefore more water molecules on average within that solvation shell than any of the polar solvents (Fig. 6).

The interactions of the various solvents with the phosphate groups in the DMPC head group are summarised in Fig. 5b. The magnitude of the first solvation peak varies amongst the various solvents, however the distance to the first minimum is identical for all of the diols (4.55 Å), which is very similar to that for water (4.45 Å). In this case, hydrogen bonding will be an important type of interaction between the solvents and the oxygens in the phosphate group, which leads to all solvents having very similar first solvation shell distances. However, there are interesting differences when considering the second solvation shell for the various solvents. The diols which have their hydroxyl groups on adjacent carbons (1,2-ethanediol, 1,2-propanediol and 1,2-butanediol) all have second solvation shell distances out to 7.55 Å, while 1,3-propanediol and 1,4-butanediol, which are longer diol molecules and have their hydroxyl groups on the terminal carbons, both have a second solvation shell distance of 7.05 Å. Therefore there is a correlation to the spacing and position of the hydroxyl groups on a diol molecule and the arrangement of the solvent molecules within the second solvation shell around the phosphate groups.

Finally, the solvation of the double-bonded carbon in the ester groups of the DMPC lipids is summarised in Fig. 5c. In this case, we can see a clear correspondence between both the length of the hydrocarbon chain of the diols and the distribution of the hydroxyl groups within the molecules and the magnitude of the first peak of the rdfs. Both 1,2-ethanediol and 1,2-propanediol, which are two of the smallest diols we have studied, and have their hydroxyl groups on adjacent carbons, have the two largest peaks, followed by 1,2-butanediol, which, while being amongst the largest diol molecule we have studied, has its hydroxyl groups on adjacent carbons. The other three diols, which all have at least one carbon separating their hydroxyl groups, all have nearly identical magnitudes of the first peak of their rdfs. As was the case for their interactions with the phosphate group, the first minimum for all of the diols are identical. Also of note is that around the ester groups it seems that while there are differing amounts of the various solvents in the second solvation shells the definition of the second solvation shell (e.g. distance corresponding to the second minimum) is very similar for all of the diols. However, the interaction of water with the ester group is significantly different. One difference is that there is a first hydration shell found in the rdf of water found at 3.45 Å. At this same distance in the rdfs of 1,2-ethanediol and 1,2-propanediol, we see a slight shoulder in the curve, and for the other diols we see a significant change in slope of the rdfs. Then the second minimum of the water rdf is found at the same distance as the first minimum of the rdfs for the diol molecules.

In order to attempt to summarise the relative solvation of each of the different groups when interacting with the various solvents, we measured the coordination number of solvent molecules around the nitrogen atom in the choline group (at a distance of 5.25 Å), around the phosphorus atom in the phosphate group (at a distance of 4.55 Å) and around the carbonyl oxygen in the ester groups (at a distance of 5.35 Å) for the DMPC molecules in the monolayers interacting with each solvent. We have plotted these results in Fig. 6. In this figure, we see the expected trend that the number of solvent molecules around the various groups reduces as we get closer to the hydrophobic/hydrophilic interface of the monolayers, as the volume available to the solvents decreases. Also, we find more water molecules within the first solvation shell of each of the different regions of the lipid head group than are present when considering any of the diol molecules. In terms of the diols, 1,2-ethanediol seems to solvate all parts of the lipid head group more than any of the other solvents we have investigated. Amongst each of these three groups of the lipid head group, the largest difference in the amount of solvation by 1,2-ethanediol and the other solvents is observed around the ester group (where there are about twice as many 1,2-ethanediol molecules than any other solvent). Interestingly, we see that 1,2-propanediol, which results in a monolayer that has a structure similar to that observed for lipids in 1,2-ethanediol, has the second largest amount of solvation around the ester groups. When considering the solvation by 1,2-propanediol around the other groups, we observe the smallest number of molecules around the choline group and the phosphate group within the PC head group of any of the solvents investigated. Whereas the second largest number of solvent molecules found around the choline and phosphate groups amongst the diols is due to 1,3-propanediol. Therefore the ability to solvate the two charged groups of the lipid head group appears to be dependent not only on the size of the solvent molecule but also the location of the hydroxyls within the molecule. While 1,2-ethanediol, 1,2-propanediol and 1,2-butanediol all have hydroxyls on adjacent carbons, 1,2-ethanediol and 1,2-propanediol are smaller than 1,2-butanediol and therefore are found to be most present around the various parts of the DMPC head group. Meanwhile, the ability of a diol to penetrate the head group region of a lipid membrane results in the potential disruption of the membrane itself.

The orientations of the solvent molecules have been measured by determining the angle that the vector connecting the two oxygen atoms in each diol and the vector normal to the interface of the DMPC monolayers, θ. Meanwhile for the water molecules we have calculated the angle between one of the O-H bond vectors and the vector normal to the interface of the DMPC monolayers. Fig. 7 shows the distribution of the $\cos\theta$ as a function of the distance in the z-dimension from the double bonded oxygen in the ester groups of the tails of the DMPC lipid molecules, where positive Δz values would represent the solvent being in the hydrophobic tails of the monolayer and negative values represent moving further into the solvent phase. Generally, we observe that the diols with hydroxyl groups on the terminal carbons (1,4-butanediol, 1,3-propanediol and 1,2-ethanediol) have two preferred orientations, one at $\cos\theta \sim 1$ and the other at $\cos\theta \sim -1$ which correspond to them being aligned parallel to the normal vector with

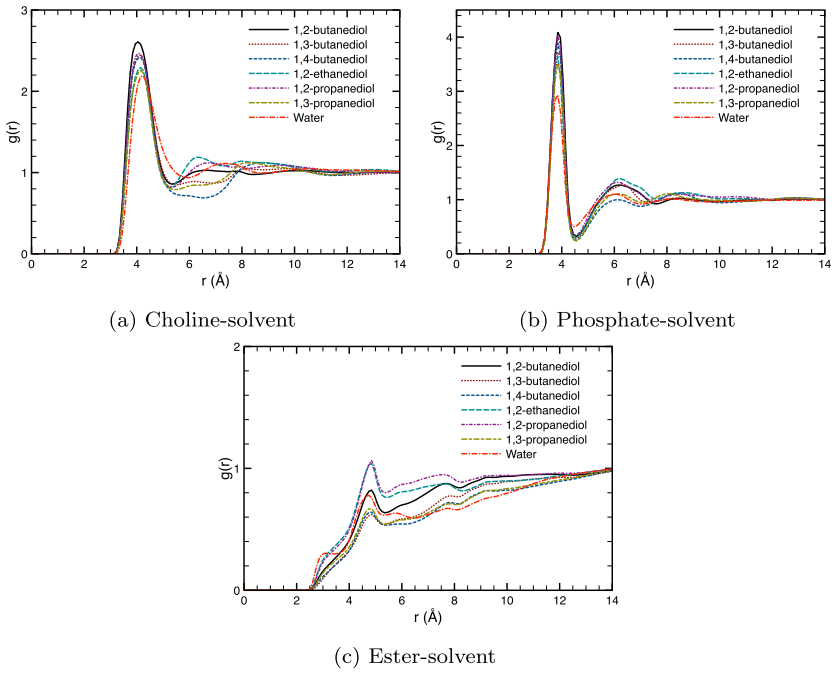

(a) Choline-solvent (b) Phosphate-solvent

(c) Ester-solvent

Fig. 5. Radial distribution functions of the oxygen atom in the hydroxyl groups of the various solvent molecules around the (a) choline, (b) phosphate and (c) ester groups of the DMPC head group.

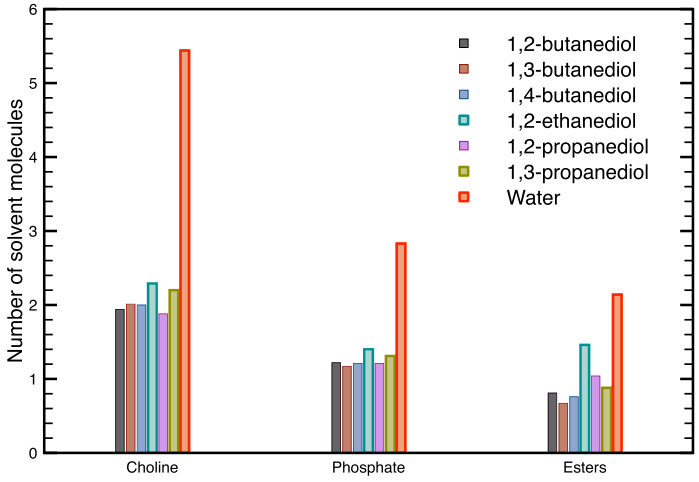

Fig. 6. Average number of solvent molecules around the choline, phosphate and ester groups within the DMPC head group region for the monolayers interacting with each of the different solvents.

either hydroxyl group oriented nearest the ester groups. Meanwhile those diols with a hydroxyl group on one of their terminal carbons have a preferential orientation such that the solvent molecule is oriented parallel to the normal vector with the hydroxl group nearest to the ester group. In water, the molecules have a preference once again to orient such that their O-H groups are oriented near the ester groups. Therefore, as expected, in all cases the solvent molecules prefer to orient such that they can form hydrogen bonds with the double-bonded oxygens in the ester groups. Note, that due to the choice of a single O-H bond as the definition of the angle there is an assymmetry as a function of $\cos\theta$ within the plot. Also the larger densities of water and 1,2-ethanediol observed in their orientation plots are consistent the solvation results shown previously.

3.7. Chains of hydrogen bonded solvent molecules

In order to investigate the role that the solvent molecules play in the interactions of the head groups of the DMPC molecules, we have mapped out the hydrogen bond networks that exist between the various solvent molecules which form continuous paths between head groups. Fig. 8 shows the probability distribution of how many of each of the different solvent molecules are found to link head groups within the same monolayer. In general, the common trend is that those solvents which result in more compressed and ordered membranes (water, 1,2-butanediol, 1,3-butanediol, 1,4-butanediol & 1,3-propanediol) are able to form short paths (less than 5 molecules) that link the different parts of the lipid head groups. Whereas for those solvents which result in less compressed and more disordered membranes (1,2-ethanediol and 1,2-propanediol), we see the least amount of short

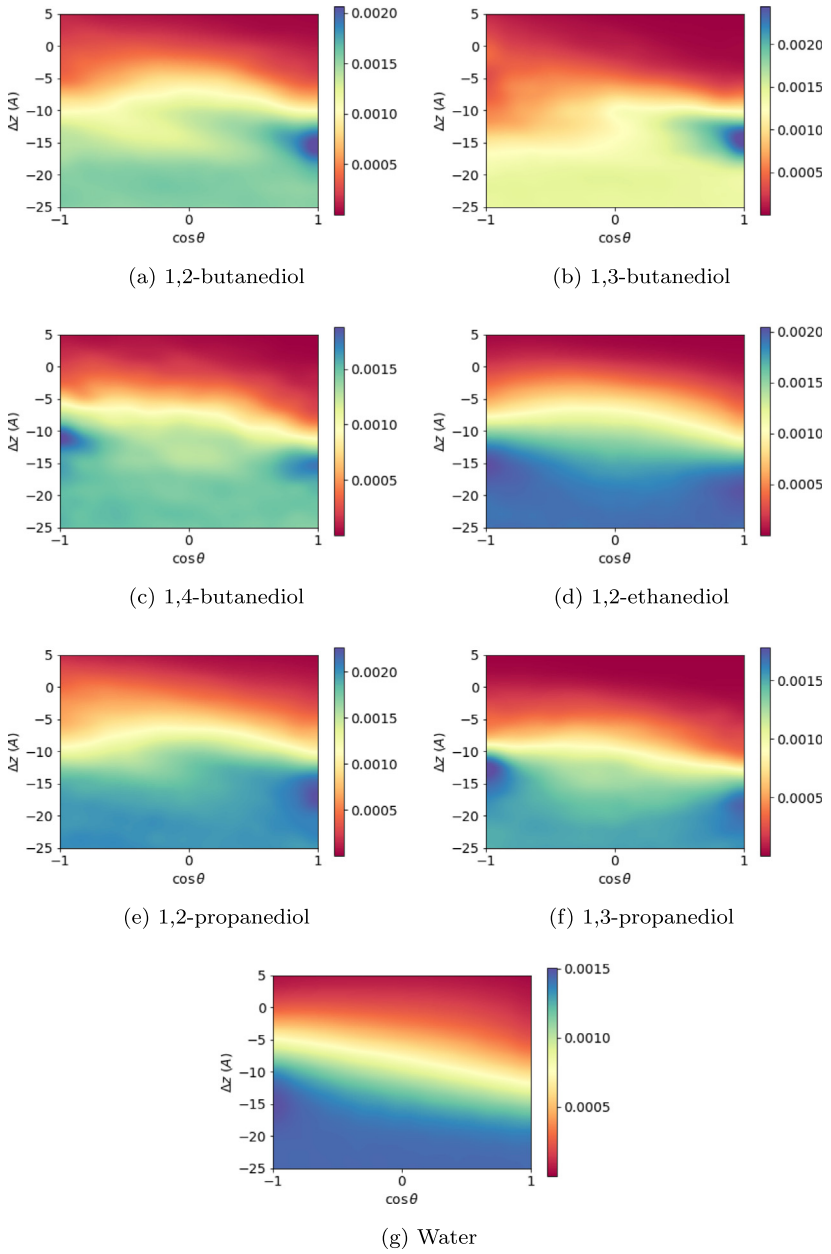

Fig. 7. Orientation of the various solvent molecules with respect to the *z*-axis as a function of distance in the *z*-dimension from the ester moieties of the DMPC lipids.

paths between any of the pairs of atoms within the PC head groups, and we see a first peak in the probability at ∼ 15 solvent molecules.

Water has a strong preference to form short hydrogen bonded chains of molecules between the various regions of the PC head group in neighbour lipid molecules, and there is a significant decay in the probability of chains existing containing larger numbers of water molecules. For the diols, however, as noted above, we see the occurance of small hydrogen bonded chains for some of the diols, but they all also form longer chains of molecules that connect the various head group regions. In the case of the diols with 2 or 3 carbons, we see that the most common number of molecules in a hydrogen-bonded chain is approximately the same for 1,2-ethanediol and 1,2-propanediol but then is larger for 1,3-propanediol. Therefore, as the hydroxyl groups become further apart the solvents need to include more molecules in chains connecting the various parts of the lipid head group. However, in the butanediols, we observe that the most probable hydrogen bonded chain length is largest for 1,3-butanediol, second largest for 1,2-butanediol, and then shortest for 1,4-butanediol, such that the most probable chain length for 1,4-butanediol is quite similar to that for 1,2-propanediol and 1,2-ethanediol, while the value for 1,2-butanediol is quit similar to 1,3-propanediol.

Of those solvents that lend themselves to forming small chains of solvent molecules between the various parts of the DMPC head groups, 1,3-butanediol has the largest probability to form small chains while also forming the longest long chains. In order to understand the cause of this behaviour we have taken a closer look at the interactions between the different butanediol solvent molecules, and have generated spatial density maps of the interactions between the two alcohol groups in the three different butanediol species (Fig. 9). (The SDMs for the three other diols are shown in Fig. S47). In these plots, it is clear that all three solvents see interactions between the two alcohol groups in the same spatial regions. However, 1,3-butanediol interacts with each other

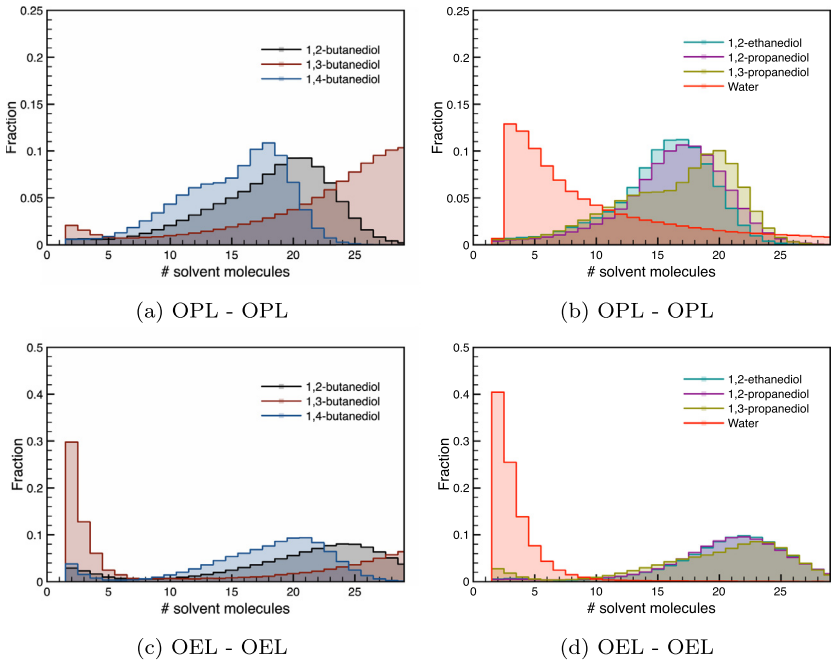

Fig. 8. Fraction of chains formed of hydrogen-bonded solvent molecules that are a given number of solvent molecules long for the interactions between the (a) & (b) OPL - OPL and (c) & (d) OEL - OEL groups in the DMPC head groups. Each of the different solvents is represented within each plot.

through OH1-OH2 hydrogen bonds almost exclusively whereas 1,2-butanediol and 1,4-butanediol have a more even distribution of OH1-OH2, OH1-OH1 and OH2-OH2 hydrogen bonds. Interestingly 1,4-butanediol which forms the shorter paths of these three diols shows equal probability of forming hydrogen bonds between any pair of diols, whereas 1,2-butanediol which forms chains of solvents of lengths in between those oberved with the other two butanediols, shows a slight preference for forming hydrogen bonds between OH1-OH1 and OH2-OH2 pairs. Therefore 1,3-butanediol will form much less branched networks of hydrogen bonded molecules whereas the 1,4-butanediol species will be able to form a significantly branched network, and this results in the various chain lengths of hydrogen bonded solvent molecules that mediate the interactions between neighbouring PC head groups.

4. Conclusions

We have carried out a series of all-atom molecular dynamics simulations in order to investigate how the chain length and distribution of hydroxyl groups within diol molecules affect the interfacial and structural properties of DMPC lipid monolayers. We showed that 1,2-ethanediol and 1,2-propanediol have the largest impact on the structure of the lipid monolayers, causing the area per lipid to increase, the monolayer thickness to decrease, and the lipid order to decrease, in comparison to that observed when the DMPC monolayers interacted with the other diols. A previous molecular dynamics simulation investigation of the effect of increasing concentrations of 1,2-ethanediol and 1,2-propanediol in an aqueous solution reported that at higher concentrations both solvents increase the area per lipid and decrease the thickness of a DPPC bilayer [17], which generally agrees with what is observed here.

In an attempt to gain an understanding of what leads to 1,2-ethanediol and 1,2-propanediol disrupting the DMPC membranes while the other diols do not, we explored the solvation properties for each solvent around the lipid head group. Generally, we find that all of the diol solvents studied interact twice as much with the choline group in the PC head group than with the phosphate group. Then in the case of 1,3-propanediol, 1,2-butanediol, 1,3-butanediol and 1,4-butanediol there is a further reduction in interaction with the ester groups of the lipids. However, 1,2-ethanediol and 1,2-propanediol are the only two solvents which have on average at least one solvent molecule interacting with the ester groups of the DMPC molecules. So it would seem that their smaller size and the distribution of the -OH groups on neighbouring carbons allows them to penetrate that much deeper into the head group region than the other solvents.

We also explored the nature of the hydrogen bonded networks of solvent groups in between the PC head groups for each of the solvents. We found that those solvents which do not disrupt the lipid membranes (1,3-propanediol, 1,2-butanediol, 1,3-butanediol, 1,4-butanediol) are able to form short (less than 5 molecule-long) hydrogen bond chains between the lipid head groups, much like water does. Meanwhile we found that for those solvents that increased the area per lipid, the short hydrogen bonded networks are not prevalent and in general there is a lot larger network which forms between the lipid head groups.

Our results show a significant dependence of the structural and interfacial properties of the DMPC monolayers on the chain length and distribution of -OH groups on diols. In a previous experimental investigation of the effect of polyols on DMPC lipid monolayers, Budziak et al. also found that the shorter polyols have the largest effect on the area per molecule and thickness of the monolayer and provided evidence that this was due to their ability to penetrate deeper into the head group region of the monolayers. [25] In addition to size, our results suggest that if the -OH groups are covalently closer to one another it also provides a greater ability for the solvent molecules to penetrate the head group region of the monolayer and thereby to disrupt the membrane stability.

Declaration of Competing Interest

The authors declare that they have no known competing financial interests or personal relationships that could have appeared to influence the work reported in this paper.

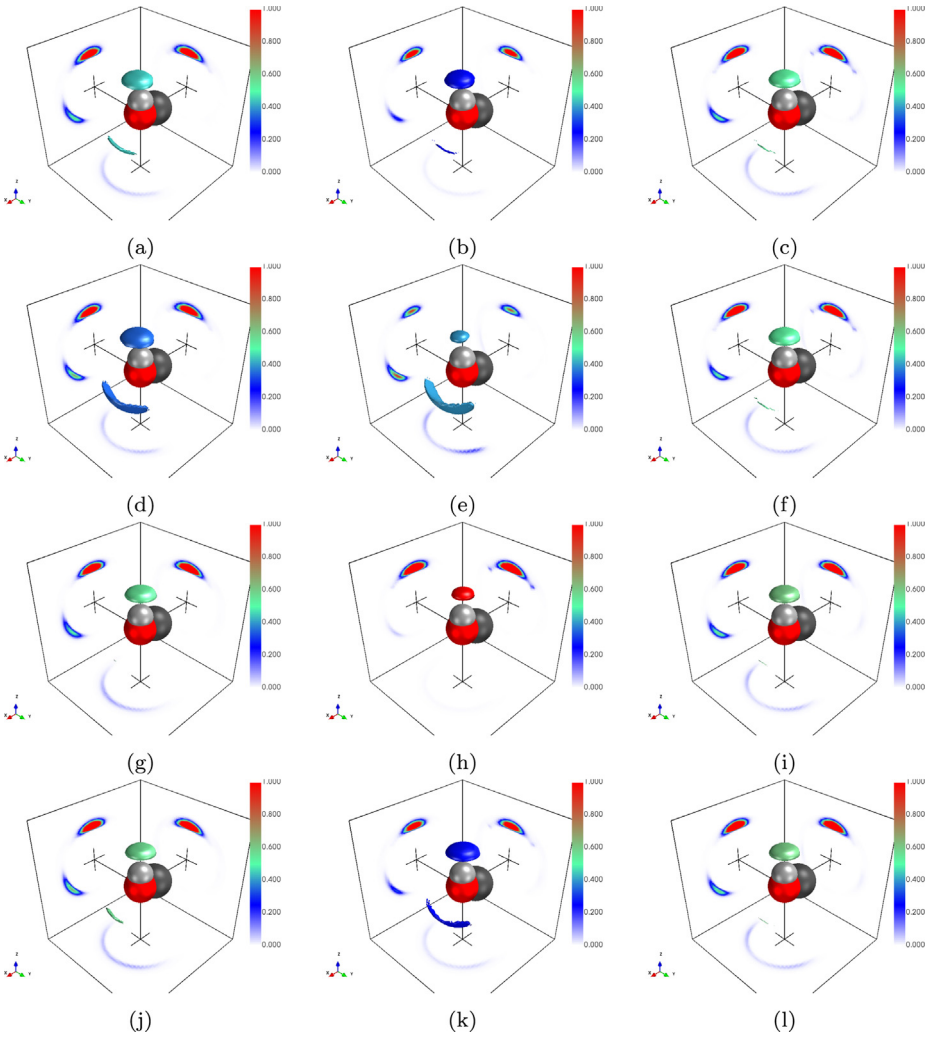

Fig. 9. Spatial density maps of the interactions between the different alcohol groups within the 1,2-butanediol, 1,3-butanediol and 1,4-butanediol molecules (from left to right): (a)-(c) OH1-OH1, (d)-(f) OH1-OH2, (g)-(i) OH2-OH1 and (j)-(l) OH2-OH2. The isopycnic surface represents 30% of solvent molecules in the first coordination shell, where the scale bar represents the density in atoms per Å^3.

Appendix A. Supplementary material

Supplementary data associated with this article can be found, in the online version, at https://doi.org/10.1016/j.molliq.2022.119963.

References

[1] M.C. Rheinstädter, T. Seydel, F. Demmel, T. Salditt, Molecular motions in lipid bilayers studied by the neutron backscattering technique, Phys. Rev. E 71 (2005) 061908.
[2] F. Foglia, M.J. Lawrence, C.D. Lorenz, S.E. McLain, On the hydration of the phosphocholine headgroup in aqueous solution, J. Chem. Phys. 133 (14) (2010) 145103.
[3] M.L. Berkowitz, R. Vácha, Aqueous solutions at the interface with phospholipid bilayers, Acc. Chem. Res. 45 (1) (2012) 74–82.
[4] S. Roy, S.M. Gruenbaum, J.L. Skinner, Theoretical vibrational sum-frequency generation spectroscopy of water near lipid and surfactant monolayer interfaces, J. Chem. Phys. 141 (18) (2014) 18C502.
[5] S. Re, W. Nishima, T. Tahara, Y. Sugita, Mosaic of water orientation structures at a neutral zwitterionic lipid/water interface revealed by molecular dynamics simulations, J. Phys. Chem. Lett. 5 (24) (2014) 4343–4348.
[6] R.J. Gillams, C.D. Lorenz, S.E. McLain, Comparative atomic-scale hydration of the ceramide and phosphocholine head group in solution and bilayer environments, J. Chem. Phys. 144 (22) (2016) 225101.
[7] N.H. Rhys, I.B. Duffy, C.L. Snowden, C.D. Lorenz, S.E. McLain, On the hydration of dope in solution, J. Chem. Phys. 150 (11) (2019) 115104.
[8] Y. Luo, G. Zhou, L. Li, S. Xiong, Z. Yang, X. Chen, L. Huang, Hydrogen bond-induced responses in mid- and far-infared spectra of interfacial water at phospholipid bilayers, Fluid Phase Equilib. 518 (2020) 112626.
[9] F. Martelli, J. Crain, G. Franzese, Network topology in water nanoconfined between phospholipid membranes, ACS Nano 14 (7) (2020) 8616–8623.
[10] T.J. McIntosh, A.D. Magid, S.A. Simon, Range of the solvation pressure between lipid membranes: Dependence on the packing density of solvent molecules, Biochemistry 28 (1989) 7904–7912.
[11] S.J. Li, K. Kinoshita, S. Furuike, M. Yamazaki, Effects of solvents interacting favorably with hydrophilic segments of the membrane surface of phosphatidylcholine on their gel-phase membranes in water, Biophys. Chem. 81 (1999) 191–196.
[12] H. Pfeiffer, R. Winter, G. Klose, K. Heremans, Thermotropic and piezotropic phase behaviour of phospholipids in propanediols and water, Chem. Phys. Lett. 371 (2003) 670–674.
[13] R. Notman, M. Noro, B. O'Malley, J. Anwar, Molecular basis for dimethylsulfoxide (dmso) action on lipid membranes, J. Amer. Chem. Soc. 128 (43) (2006) 13982–13983.
[14] R. Notman, W.K. den Otter, M.G. Noro, W.J. Briels, J. Anwar, The permeability enhancing mechanism of dmso in ceramide bilayers simulated by molecular dynamics, Biophys. J. 93 (6) (2007) 2056–2068.
[15] A.P. Dabkowska, F. Foglia, M.J. Lawrence, C.D. Lorenz, S.E. McLain, On the solvation structure of dimethylsulfoxide/water around the phosphatidylcholine head group in solution, J. Chem. Phys. 135 (22) (2011) 225105.
[16] A.P. Dabkowska, M.J. Lawrence, S.E. McLain, C.D. Lorenz, On the nature of hydrogen bonding between the phosphatidylcholine head group and water and dimethylsulfoxide, Chem. Phys. 410 (2013) 31–36.
[17] C.J. Malajczuk, Z.E. Hughes, R.L. Mancera, Molecular dynamics simulations of the interactions of dmso, mono- and polyhydroxylated cryosolvents with a

hydrated phospholipid bilayer, Biochim. Biophys. Acta 2013 (1828) 2041–2055.
[18] A.P. Dabkowska, L.E. Collins, D.J. Barlow, R. Barker, S.E. McLain, M.J. Lawrence, C.D. Lorenz, Modulation of dipalmitoylphosphatidylcholine monolayers by dimethyl sulphoxide, Langmuir 30 (29) (2014) 8803–8811.
[19] Z.E. Hughes, R.L. Mancera, Molecular mechanism of the synergistic effects of vitrification solutions on the stability of phospholipid bilayers, Biophys. J. 106 (2014) 2617–2624.
[20] R.J. Gillams, J.V. Busto, S. Busch, F.M. Goni, C.D. Lorenz, S.E. McLain, Solvation and hydration of the ceramide headgroup in a non-polar solution, J. Phys. Chem. B 119 (1) (2015) 128–139.
[21] R. Thind, D.W. O'Neill, A.D. Regno, R. Notman, Ethanol induces the formation of water-permeable defects in model bilayers of skin lipids, Chem. Comm. 51 (25) (2015) 5406–5409.
[22] S. Nakata, A. Deguchi, Y. Seki, M. Furuta, K. Fukuhara, S. Nishihara, K. Inoue, N. Kumazawa, S. Mashiko, S. Fujihira, M. Goto, M. Denda, Characteristic responses of a phospholipid molecular layer to polyols, Colloids Surf. B 136 (2015) 594–599.
[23] N.H. Rhys, M.A. Al-Badri, R.M. Ziolek, R.J. Gillams, L.E. Collins, M.J. Lawrence, C. D. Lorenz, S.E. McLain, On the solvation of the phosphocholine headgroup in an aqueous propylene glycol solution, J. Chem. Phys. 148 (13) (2018) 135102.
[24] W. Terakosolphan, J.L. Trick, P.G. Royall, S.E. Rogers, O. Lamberti, C.D. Lorenz, B. Forbes, R.D. Harvey, Glycerol solvates dppc headgroups and localises in the interfacial regions of model pulmonary interfaces altering bilayer structure, Langmuir 34 (23) (2018) 6941–6954.
[25] I. Budziak, M. Arczewska, M. Sachadyn-Król, A. Matwijczuk, A. Wako, M. Gago, K. Terpilöwski, D.M. Kamiński, Effect of polyols on the dmpc lipid monolayers and bilayers, Biochim. Biophys. Acta Biomembr. 1860 (2018) 2166–2174.
[26] R. Raju, J. Torrent-Burgues, G. Bryant, Interactions of cryoprotective agents with phospholipid membranes – a langmuir monolayer study, Chem. Phys. Lipids 231 (2020) 104949.
[27] C.S. Pereira, P.H. Hunenberger, The influence of polyhydroxylated compounds on a hydrated phospholipid bilayer: a molecular dynamics study, Mol. Simul. 34 (2008) 403–420.
[28] J.H. Crowe, L.M. Crowe, J.F. Carpenter, A.S. Rudolph, C.A. Wistrom, B.J. Spargo, T.J. Anchordoguy, Interactions of sugars with membranes, Biochim. Biophys. Acta 947 (2) (1988) 367–384.
[29] W.L. Dills, Sugar alcohols as bulk sweetners, Annu. Rev. Nutr. 9 (1989) 161–186.
[30] P. Westh, Unilamellar dmpc vesicles in aqueous glycerol: Preferential interactions and thermochemistry, Biophys. J. 84 (1) (2003) 341–349.
[31] O. Akinterinwa, R. Khankal, P.C. Cirino, Metabolic engineering for bioproduction of sugar alcohols, Curr. Opin. Biotechnol. 19 (5) (2008) 461–467.
[32] A. Kyrychenko, T.S. Dyubko, Molecular dynamics simulations of microstructure and mixing dynamics of cryoprotective solvents in water and in the presence of a lipid membrane, Biophys. Chem. 136 (1) (2008) 23–31.
[33] A. Nowacka, S. Douezan, L. Wadso, D. Topgaard, E. Sparr, Small polar molecules like glycerol and urea can preserve the fluidity of lipid bilayers under dry conditions, Soft Matter 8 (5) (2012) 1482–1491.
[34] K. Asare-Addo, B.R. Conway, M.J. Hajamohaideen, W. Kaialy, A. Nokhodchi, H. Larhrib, Aqueous and hydro-alcoholic media effects on polyols, Colloids Surf. B 111 (2013) 24–29.
[35] E. Bielski, Q. Zhong, H. Mirza, M. Brown, A. Molla, T. Carvajal, S.R.P. da Rocha, Tpp-dendrimer nanocarriers for sirna delivery to the pulmonary epithelium and their dry powder and metered-dose inhaler formulations, Int. J. Pharm. 527 (1–2) (2017) 171–183.
[36] S. Ni, Y. Liu, Y. Tang, J. Chen, S. Li, J. Pu, L. Han, Gaba$_B$ receptor ligand-directed trimethyl chitosan/tripolyphosphate nanoparticles and their pmdi formulation for survivin sirna pulmonary delivery, Carbohydr. Polym. 179 (2018) 135–144.
[37] A.N. Dickey, R. Faller, How alcohol chain-length and concentration modulate hydrogen bond formation in a lipid bilayer, Biophys. J. 92 (7) (2007) 2366–2376.
[38] T. Kondela, J. Gallova, T. Hauss, J. Barnoud, S.J. Marrink, N. Kucerka, Alcohol interactions with lipid bilayers, Molecules 22 (12) (2017) 2078.
[39] S. Jo, T. Kim, V.G. Iyer, W. Im, Charmm-gui: A web-based graphical user interface for charmm, J. Comput. Chem. 29 (11) (2008) 1859–1865.
[40] S. Jo, J.B. Lim, J.B. Klauda, W. Im, Charmm-gui membrane builder for mixed bilayers and its application to yeast membranes, Biophys. J. 97 (1) (2009) 50–58.
[41] E.L. Wu, X. Cheng, S. Jo, H. Rui, K.C. Song, E.M. Dàvila-Contreras, Y. Qi, J. Lee, V. Monje-Galvan, R.M. Venable, J.B. Klauda, W. Im, Charmm-gui membrane builder toward realistic biological membrane simulations, J. Comput. Chem. 35 (27) (2014) 1997–2004.
[42] J. Lee, D.S. Patel, J. Støahle, S.-J. Park, N.R. Kern, S. Kim, J. Lee, X. Cheng, M.A. Valvano, O. Hoist, Y.A. Knirel, Y. Qi, S. Jo, J.B. Klauda, G. Widmalm, W. Im, Charmm-gui membrane builder for complex biological membrane simulations with glycolipids and lipoglycans, J. Chem. Theory Chem. 15 (1) (2019) 775–786.
[43] L. Martinez, R. Andrade, E.G. Birgin, J.M. Martinez, Packmol: A package for building initial configurations for molecular dynamics simulations, J. Comput. Chem. 30 (13) (2009) 2157–2164.
[44] J. Lee, X. Cheng, J.M. Swails, M.S. Yeom, P.K. Eastman, J.A. Lemkul, S. Wei, J. Buckner, J.C. Jeong, Y. Qi, S. Jo, V.S. Pande, D.A. Case, C.L.B. III, A.D.M. Jr, J.B. Klauda, W. Im, Charmm-gui input generator for namd, gromacs, amber, openmm, and charmm/openmm simulations using the charmm36 additive force field, J. Chem. Theory Comput. 12 (1) (2016) 405–413.
[45] S. Plimpton, Fast parallel algorithms for short-range molecular dynamics, J. Comp. Phys. 117 (1995) 1–19.
[46] N. Michaud-Agrawal, E.J. Denning, W.T.B., O. Beckstein, MDAnalysis: A Toolkit for the Analysis of Molecular Dynamics Simulations, J. Comput. Chem. 32 (2011) 2319–2327. doi:10.1002/jcc.21787.
[47] R.J. Gowers, M. Linke, J. Barnoud, T.J.E. Reddy, M.N. Melo, S.L. Seyler, D.L. Dotson, J. Domanski, S. Buchoux, I.M. Kenney, O. Beckstein, MDAnalysis: A Python package for the rapid analysis of molecular dynamics simulations., in: S. Benthall, S. Rostrup (Eds.), In Proceedings of the 15th Python in Science Conference, Austin, TX USA, 2016, pp. 102–109.
[48] P. Smith, C.D. Lorenz, Lipyphilic: A python toolkit for the analysis of lipid membrane simulations, J. Chem. Theory Comput. 17 (9) (2021) 5907–5919.
[49] V. Ramasubramani, B.D. Dice, E.S. Harper, M.P. Spellings, J.A. Anderson, S.C. Glotzer, freud: A software suite for high throughput analysis of particle simulation data, Comput. Phys. Commun. 254 (2020) 107275, https://doi.org/10.1016/j.cpc.2020.107275.
[50] P. Smith, R.M. Ziolek, E. Gazzarrini, D.M. Owen, C.D. Lorenz, On the interaction of hyaluronic acid with synovial fluid lipid membranes, Phys. Chem. Chem. Phys. 21 (19) (2019) 9845–9857, https://doi.org/10.1039/c9cp01532a, URL https://pubs.rsc.org/en/content/articlehtml/2019/cp/c9cp01532a https://pubs.rsc.org/en/content/articlelanding/2019/cp/c9cp01532a.
[51] https://gcm.upc.edu/en/members/luis-carlos/angula/angula.
[52] S. Busch, C.D. Lorenz, J. Taylor, L.C. Pardo, S.E. McLain, Short-range interactions of concentrated proline in aqueous solution, J. Phys. Chem. B 118 (49) (2014) 14267–14277, https://doi.org/10.1021/jp508779d.
[53] N.H. Rhys, R.J. Gillams, L.E. Collins, S.K. Callear, M.J. Lawrence, S.E. McLain, On the structure of an aqueous propylene glycol solution, J. Chem. Phys. 145 (22) (2016) 224504, https://doi.org/10.1063/1.4971208.
[54] K. Tanaka, P.A. Manning, V.K. Lau, H. Yu, Lipid lateral diffusion in dilauroylphosphatidylcholine/cholesterol mixed monolayers at the air/water interface, Langmuir 15 (1999) 600–606.
[55] A.A. Gurtovenko, M. Patra, M. Karttunen, I. Vattulainen, Cationic dmpc/dmtap lipid bilayers: Molecular dynamics study, Biophys. J. 86 (6) (2004) 3461–3472.
[56] N. Ganesan, B.A. Bauer, T.R. Lucas, S. Patel, M. Taufer, Structural, dynamic, and electrostatic properties of fully hydrated dmpc bilayers from molecular dynamics simulations accelerated with graphical processing units (gpus), J. Comput. Chem. 32 (14) (2011) 2958–2973.
[57] T.R. Lucas, B.A. Bauer, J.E. Davis, S. Patel, Molecular dynamics simulation of hydrated dppc monolayers using charge equilibration force fields, J. Comput. Chem. 33 (2012) 141–152.
[58] H. Dominguez, A.M. Smondyrev, M.L. Berkowitz, Computer simulations of phosphatidylcholine monolayers at air/water and ccl4/water interfaces, J. Phys. Chem. B 103 (1999) 9582–9588.
[59] D. Mohammad-Aghaie, E. Mace, C.A. Sennoga, J.M. Seddon, F. Bresme, Molecular dynamics simulations of liquid condensed to liquid expanded transitions in dppc monolayers, J. Phys. Chem. B 114 (2010) 1325–1335.
[60] H. Mohwald, Phospholipid and phospholipid-protein monolayers at the air/water interface, Annu. Rev. Phys. Chem. 41 (1990) 441–476.
[61] G. Ma, H.C. Allen, Dppc langmuir monolayer at the air-water interface: Probing the tail and head groups by vibrational sum frequency generation spectroscopy, Langmuir 22 (2006) 5341–5349.